MICROMECHANICS OF FATIGUE IN WOVEN AND STITCHED COMPOSITES

B.N. Cox, M.S. Dadkhah, R.V. Inman,
M.R. Mitchell, W.L. Morris, and S. Schroeder

Rockwell International Science Center
1049 Camino Dos Rios
Thousand Oaks, CA

Summary

The goal of this basic research program is to determine how microstructural factors, especially the architecture of reinforcing fibers, control fatigue damage in 3D reinforced polymer composites.

Test materials are being fabricated from various preforms, including stitched quasi-isotropic laminates; and through-the-thickness angle interlock, layer-to-layer angle interlock, and through-the-thickness stitching effect weaves. Preforms are impregnated with a tough resin by a special vacuum infiltration method. Careful control of this process and the cure cycle is necessary to obtain specimens free of bubbles and cracks.

Most tests are being performed in uniaxial compression/compression loading. In all cases to date, failure has occurred not by delamination (as in a 2D composite) but by shear failure, which occurs suddenly rather than by gradual macroscopic crack growth.

Special apparatus has been set up to enable optical images of the gauge section to be captured, digitized, and stored at various epochs in the fatigue life. These images are subsequently analyzed by our unique high accuracy strain mapping instrument, HASMAP, to reveal the evolution of strain fields during fatigue. The strain fields are measured with sufficient resolution to illuminate micromechanical events on the scale of individual fiber tows. They reveal the subtle damage that foreshadows eventual failure.

Some theoretical aspects of bridging effects have also been examined, especially the role of the bridging length scale, which is the increment of crack growth over which bridging by 3D tows becomes effective. Among other things, these considerations reveal why impact damage can be such a strong function of specimen size and shape.

MATERIAL MATRIX

Preforms

Most preforms in the material matrix are either woven fiber mats supplied by Textile Technologies Inc. (TTI - Hatboro, Pennsylvania) or stitched quasi-isotropic laminates supplied by HiTech/Hexcel Inc. (Reno, Nevada). They are described in the following table. The TTI preforms vary in thickness from 0.35" to 0.5", while each Hexcel panel is approximately 5/16" thick.

Table 1
Preform Matrix

Woven preforms from TTI:

Panel	Weave Pattern	Warp and Weft	Stitching Fiber	Approximate Dimensions
A	layer-to-layer angle interlock	AS4	AS4	38" x 4"
B	layer-to-layer angle interlock	AS4	S-glass	30" x 4"
C	through-the-thickness angle interlock	AS4	S-glass	38" x 4"
D	through-the-thickness angle interlock	AS4	AS4	38" x 4"
E	through-the-thickness stitching effect	AS4	AS4	12" x 9"
F	through-the-thickness stitching effect	AS4	E-glass	12" x 9"

Stitched preforms from Hexcel:

Panel	Stitching Pattern	Warp and Weft	Stitching Fiber	Approximate Dimensions
G	6 rows/in.	T300	S-glass	12" x 12"
H	12 rows/in.	T300	S-glass	12" x 12"
I	Two half-thickness panels each stitched at 6 rows/in.; then joined at 6 rows/in.	T300	S-glass	12" x 12"

LAYER TO LAYER
ANGLE INTERLOCK

THROUGH-THE-THICKNESS
ANGLE INTERLOCK

"STITCHING" EFFECT
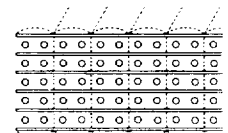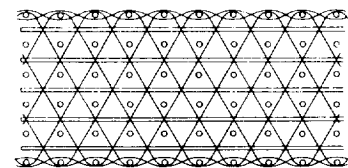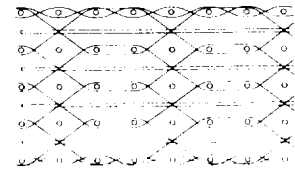
Resin

Most composites have been filled with Tactix 138 resin and H41 hardener, supplied by Dow Chemical (Freeport, Texas). A few specimens were filled early in the program with Epon 828 (Shell Chemical Co.). Since the Tactix 138 is tougher, it gives a much superior product (see "Specimen Fabrication" below).

Odd Specimens

The basic material matrix is supplemented from time to time by small specimens received from other research groups.

SPECIMEN FABRICATION

All the preforms in Table 1 are being processed in-house into composite specimens within this program. The processing route is as follows.

Impregnation and cure using Tactix 138 resin and H41 hardener (Dow Chemical) are effected in a reusable aluminum mold. The preform is placed in the mold, heated to 65°C, and degassed in a vacuum of ~1 Torr. The resin is then mixed with the hardener and also heated to 65°C and degassed. The resin mixture is then poured over the preform (still at 65°C) and the whole assembly is degassed twice again. The first degassing results in bubbling out of some volatiles followed by apparent boiling of the resin mixture as the pressure falls further. The second degassing pass produces very little emission of volatiles down to the pressure at which boiling began on the first degassing, where the degassing is now stopped. The mold is then closed and the specimen cured, the curing cycle (which is chosen to maximize resin toughness) comprising 2 hrs at 120°C and 2 hrs at 177°C. All fabrication runs to date have produced 10"x4" panels, from which 12-16 rectangular fatigue specimens can be machined.

In contrast to specimens cured with the more brittle resin Epon 828, in which extensive microcracking was found emanating from interior sites where glass interlock tows abutted AS4 warp or weft tows, the specimens cured with Tactix 138 are almost entirely free of microcracks. The only microcracks found are in surface resin layers. If excess resin is allowed to cure outside the preform, large, regularly spaced cracks will form in it. If care is taken to avoid excess resin (which is not especially easy for the TTI preforms, whose thickness varies), microcracks are still occasionally found in surface pockets of resin between tows (Fig. 1). Such microcracks extend into the composite until they encounter the internal microstructure. Thus their average size is about the diameter of one fiber tow. The large openings of these cracks attest to the substantial residual stresses in the epoxy that evidently drive the microcracking.
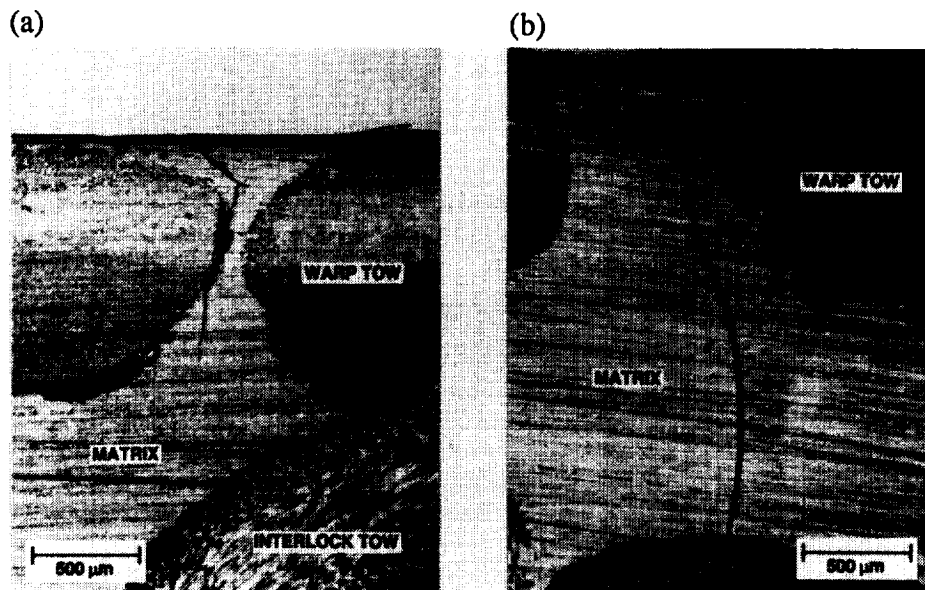
(a)   (b)

Fig. 1   Two surface microcracks found in a composite of Tactix 138/H41 and preform from panel D of Table 1.

ASSESSMENT OF PREFORM INFILTRATION

Fabricated composites have been sectioned and polished perpendicular and parallel to the warp fibers to allow porosity and fiber volume fractions to be estimated. Figure 2(a) shows an optical micrograph of a typical section through a through-the-thickness angle interlock composite (panel D of Table 1). There is no visible porosity. Figure 2(b) shows an SEM micrograph of a section of a single tow, in which it is clear that complete wetting of each individual fiber has occurred.

From Fig. 2(a), the volume fraction constituted by warp, weft, and interlock tows can be estimated at ~ 0.7; while from Fig. 2(b), the volume fraction of fibers within each tow is also ~ 0.7. Consequently, the net fiber volume fraction of the composite is ~ 0.5. More accurate values will be obtained from resin extraction measurements.
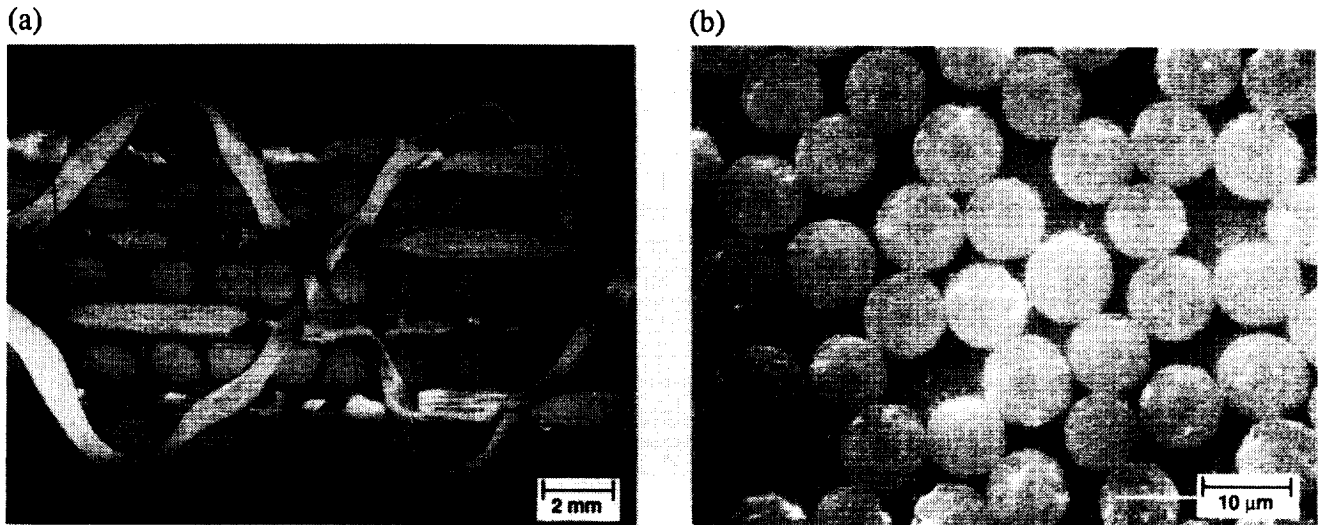
(a)

(b)

Fig. 2   (a) Optical micrograph of section parallel to warp fibers through composite of panel D of Table 1 with Tactix 138/H41 matrix. (b) SEM micrograph of section through an individual warp tow in (a).

TEST MATRIX

Macroscopic Tests

The basic test matrix consists of tests on specimens made from the preforms of Table 1. Panels fabricated as described in "Specimen Fabrication" are cut into rectangular specimens of dimensions 4" × 1/2" × panel thickness. These are being subjected to fully reversed (R = -1), tension-tension (R = 0), and compression-compression (R = -∞) uniaxial fatigue loading. For each R ratio, five load amplitudes are being covered, making a matrix of 15 tests for each material in the material matrix.

The material matrix includes the six weave types supplied by TTI and the three stitching patterns in the Hexcel panels (Table 1). Because of weave or stitching asymmetry, neither the TTI nor the Hexcel specimens possess in-plane isotropy, being instead orthotropic. Specimens are being tested with the load axis lying along both in-plane directions of reflective symmetry. The material matrix therefore comprises 18 cases.

The total number of tests in the basic matrix is accordingly 270 (15 loads × 18 materials).

Micromechanical Tests

When test results look especially significant or interesting, the micromechanics of the failure are investigated using either the actual specimens in the matrix or nominally identical ones in repeat tests. The micromechanical investigations are based primarily on HASMAP, as described on the following pages.

583

IN SITU DIGITAL IMAGE COLLECTION FOR HASMAP

HASMAP (for high accuracy strain field mapper) determines fields of differential surface deformation by comparing digital images of deformed and undeformed material. In its usual mode, HASMAP achieves very high spatial resolution by analyzing optical or SEM micrographs. The micrograph images are digitized by a CCD camera, which provides the maximum possible spatial stability. The pixel density in the digitization is increased by digitizing small areas on each micrograph at a time so that the entire micrograph is represented by arrays of between 1000 × 1000 and 4000 × 4000 pixels.

In this program, we have developed special apparatus to streamline this process by obviating the use of micrographs, opening the way to substantial decreases in labor costs and increasing the volume of data that can be analyzed. The CCD camera is placed in situ in the test apparatus (Fig. 3). It is mounted on a precise x-y-z stage, which can be scanned to obtain an array of overlapping (typically by 10%) digital images directly from the specimen surface. At 60X, the entire specimen gauge section can be covered by a 2 × 2 array of digitized images, each of which is represented by a 480 × 512 array of pixels (the intrinsic array size of the CCD camera).

While the rigid structure of the x-y-z stage ensures the absence of relative rotations between digitized images in the 2 × 2 array, relative translations are known only to within a few microns. These translational errors are computed and eliminated by calculating cross-correlations within the overlapping strip between each pair of images and adjusting their assigned positions within the computer accordingly.
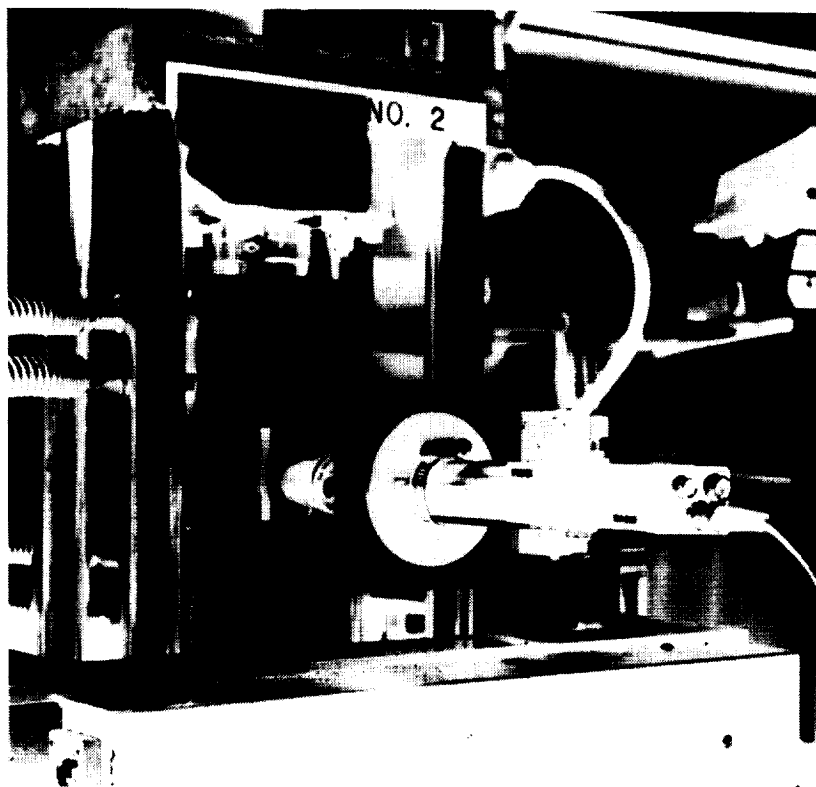

Fig. 3 Loading frame and CCD camera mounted on x-y-z stage.

DISPLACEMENT VECTORS CALCULATED BY HASMAP

The net result of the procedure described on the previous page is a digitized 1000 × 1000 pixel image of the entire specimen width over a good portion of the gauge length. Relative displacements between pairs of such images (usually recorded at constant load before and after the application of fatigue cycles) are found by high speed cross-correlation calculations. The calculations are performed over a 16 × 16 array of points, with the analysis for each point carried out over a 32 × 32 pixel image segment. The displacement accuracy of this analysis is ± 0.2 pixels, corresponding to ~ ± 0.2 μm on the specimen. (While HASMAP can achieve displacement accuracy of ± 100Å when high magnification optical micrographs are used,[1] such precision would be superfluous here. Furthermore, data must be recorded over as much of the gauge section as possible when testing smooth specimens because deformation and eventual failure can be found anywhere on it. Limitations of data storage capacity dictate that this be done at moderate magnification.)

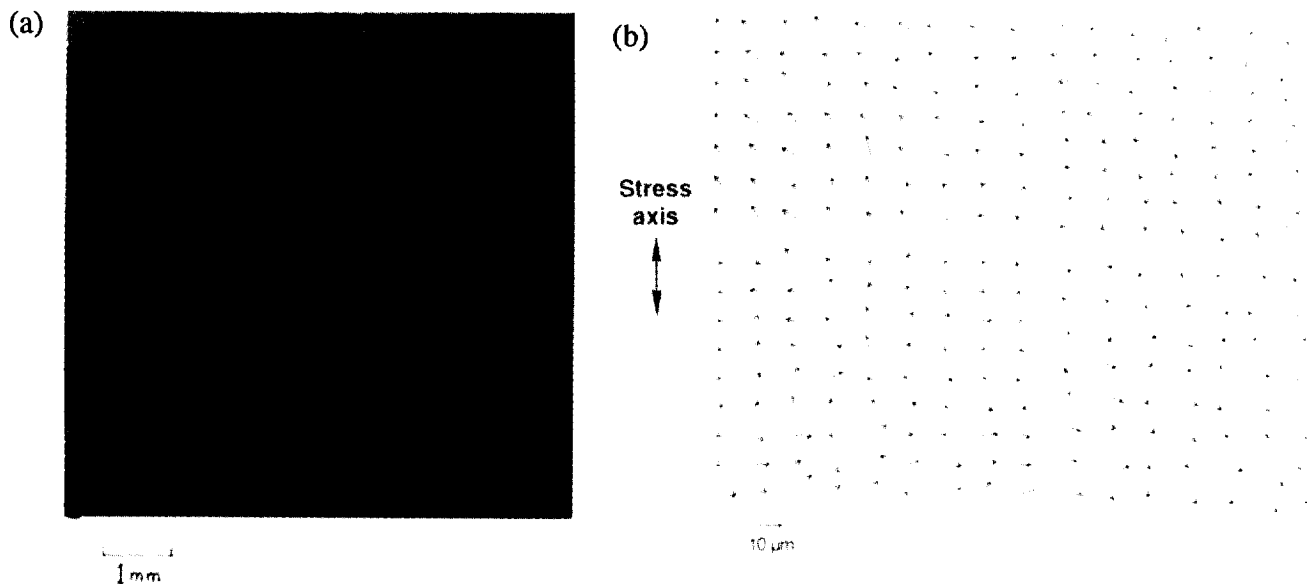A typical array of displacement vectors is shown in Fig. 4.

Fig. 4   Deformation in a stitched composite (supplied by B. Dexter, NASA Langley; not listed in Table 1) resulting from 8000 compression-compression fatigue cycles to a peak load of -260 MPa. Images were recorded at -130 MPa. (a) Digitized image of gauge section, which has been decorated with SiC particles to enhance contrast. (b) Differential displacement vector field computed for the area of (a) showing the irreversible displacements associated with fatigue damage.

---

[1]M.R. James, W.L. Morris, and B.N. Cox, "A High Accuracy Automated Strain Field Mapper," Exptl. Mech. 30, 60-67 (1990).

DISPLACEMENT AND STRAIN FIELDS FROM HASMAP

Continuous full field deformation maps are deduced from vectors such as those of Fig. 4 as follows. Contours of constant u and v (the displacements perpendicular and parallel to the sample axis) are formed by linear interpolation between values of the appropriate component of the vector array. These are then smoothed by an algorithm which dilates and then erodes each contour level, removing a prescribed amount of high frequency noise. There results a set of contours (Fig. 5(a)) which, for the present application, have a resolution comparable to high resolution moiré fringes, with the advantage over the moiré method that the absolute sense of the local deformation (i.e., whether it is compressive or tensile) is always known. The derivatives of these displacements are then taken to generate a complete set of strain fields relative either to the specimen or to the local principal stress axes as desired. Figure 5(b) shows the strain component ε_{yy} derived from Fig. 5(a), where the y-axis is the stress axis.

The zone of heavy deformation (strains ~ 10^{-2}) striking across Fig. 5(b) from center-left to center coincides with a single stitching tow, the only one falling in the field of view. Longer range deformation shows that the gauge section has also sheared during fatigue. This is clearest in Fig. 4(b): the directions of the displacement vectors at the top left and bottom right indicate tensile strain normal to the diagonal that runs from bottom left to top right. The specimen ultimately failed along this diagonal.
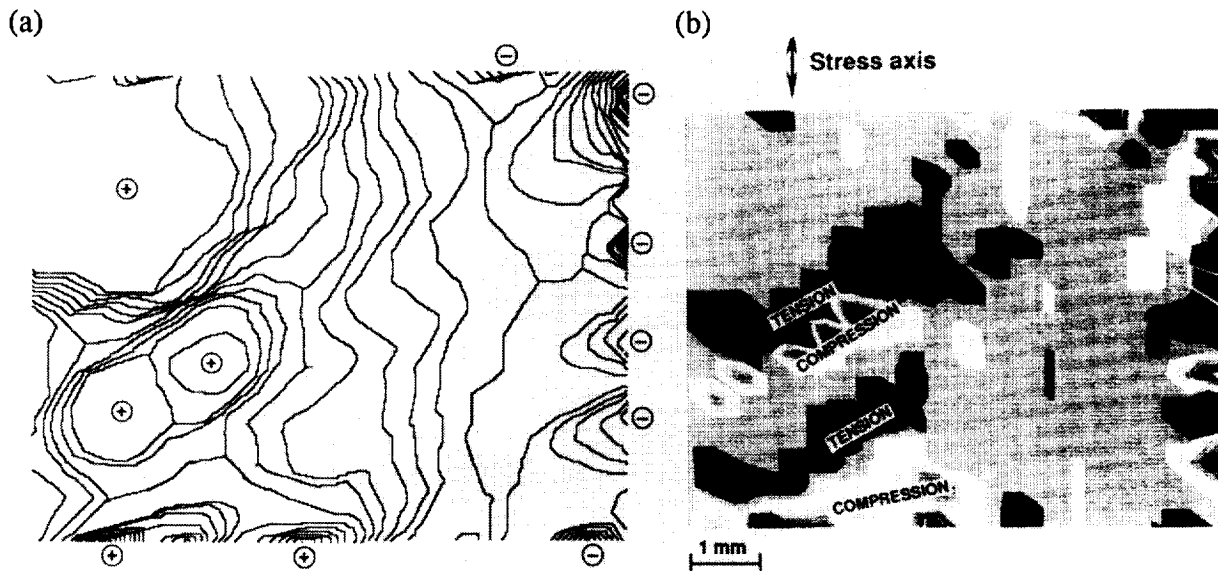

Fig. 5   (a) Contours of the displacement v (parallel to the stress axis) derived from the vectors of Fig. 4. Symbols + and - show local maxima and minima. Contours are separated by 0.6 μm in displacement. (b) The strain field ε_{yy} derived from (a). In this black and white rendition of a color image, important zones of maximum tension and compression have been labeled. Each gray level indicates a strain increment of 1.1×10^{-3}.

586

EXTRINSIC FACTORS IN CRACK BRIDGING

Crack bridging by 3D fiber tows is the primary source of macroscopic crack resistance following delamination in impact tests, and it is probably one of the key factors in preventing microscopic cracks from propagating into macroscopic cracks during fatigue of pristine material. Extensive theoretical studies of bridged cracks have recently been conducted, mainly under other funding.[2,3] This work has shown very clearly that the mechanics of bridged cracks depend strongly on extrinsic factors. In particular, the stress required to propagate a matrix crack and the transition from intact bridging ligaments (ductile failure) to ruptured ligaments (brittle failure) depend strongly on load distribution and the size of the specimen and any notch.

Within this program, the significance of these results for impact testing in 3D composites, and possibly for fatigue resistance too, has also been considered. A central role is played by the "bridging length scale," the characteristic length of initial crack growth over which the bridging zone matures.[3] This is a critical engineering property of any material containing bridged cracks. It can vary from the order of the fiber diameter to several meters, depending on the nature of the bridging ligaments. The length to which a microcrack might propagate before arresting is determined by the bridging length scale; the size of a delamination crack caused by impact will depend on how large the stressed area is relative to the bridging length scale; and whether such a bridged delamination will subsequently propagate to failure will depend on the specimen size in terms of the bridging length scale.

While no predictive theory for bridged cracks that is accurate for all load configurations and specimen sizes has yet been demonstrated, it is clear from simulations[3] that the critical information is the relation between the opening displacement u of a bridged crack and the tractions p imposed by the bridging ligaments. If $p(u)$ is not known and conventional engineering methods of fracture mechanics are applied, severely nonconservative predictions are possible. The effects discussed in Ref. 3 may account for many of the discrepancies reported for different kinds of impact tests involving specimens of different sizes and shapes.[4]

ACKNOWLEDGMENTS

[2]B.N. Cox and D.B. Marshall, "Stable and Unstable Solutions for Bridged Cracks in Various Specimens," Acta Metall., in press.

[3]B.N. Cox, "Extrinsic Factors in the Mechanics of Bridged Cracks," submitted to Acta Metall.

[4]P.E. Reed, "Impact Testing of Plastics for Design," in ATA-MAT 89, Turin, Italy, June 1989 (Associazione Tecnica Dell'automobile, Italy, 1989).